

**XRD and Laser Raman Spectroscopy Investigation
of the Stability of Low Temperature t -ZrO₂**

Goran Štefanić,^{a,*} Svetozar Musić,^a Biserka Gržeta,^a Stanko Popović,^b
and Andreja Sekulić^a

^aRuđer Bošković Institute, P. O. Box 1016, 10001 Zagreb, Croatia

^bDepartment of Physics, Faculty of Science, University of Zagreb,
P. O. Box 162, 10001 Zagreb, Croatia

Received: January 22, 1998; revised March 13, 1998; accepted May 21, 1998

The influence of precipitation pH and the presence of Na⁺ impurities on the stability of metastable t -ZrO₂ were investigated. Zirconia samples with a high t -ZrO₂ phase content were crystallized from zirconium hydroxide precipitated at pH 13, 7 and 2.5. The obtained samples were subjected to the influence of temperature, pressure and γ -irradiation. The influence of these treatments on the metastable t -ZrO₂ were investigated using XRD and laser Raman spectroscopy. The results of phase analysis showed that the change in the pH of zirconium hydroxide precipitation significantly changed the sensitivity of the metastable t -ZrO₂ to temperature and pressure. The metastable t -ZrO₂ was most stable in the sample obtained from zirconium hydroxide precipitated at pH 2.5 and most unstable in the sample obtained from zirconium hydroxide precipitated at pH 7. The presence of Na⁺ impurities decreased the stability of metastable t -ZrO₂. All the samples were shown to be stable under high γ -irradiation. The capability of laser Raman spectroscopy for the quantitative analysis was examined by comparing the values of the m -ZrO₂ volume fraction (v_m) obtained by this technique with the corresponding values obtained by XRD. It was concluded that the relation proposed by Clarke and Adar, *J. Am. Ceram. Soc.* **65** (1982) 284., was correct but the reliability of the v_m values estimated by the laser Raman spectroscopy was not high, especially in the region of $0.15 < v_m < 0.70$. The reason for the low reliability in this region is discussed.

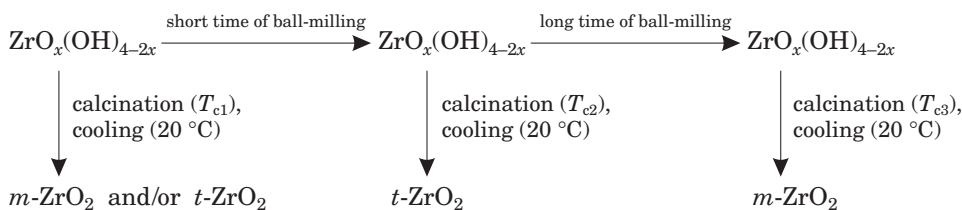
* Author to whom correspondence should be addressed.

INTRODUCTION

Martensitic transformation from tetragonal to monoclinic zirconia polymorph causes volume expansion from 3 % to 5%. This effect was used to improve the toughness of ceramic material.¹ Crack propagation generates stress in the ceramic material which can cause transformation of the small metastable $t\text{-ZrO}_2$ particles, incorporated in the bulk of the ceramic material. Volume expansion of the transformed particles generates compressive strain in the vicinity of the crack, so extra work would be required to move the crack through the ceramic material.¹ In order to obtain ceramics with improved toughness it is important to know the stability of the $t\text{-ZrO}_2$ particles. If their stability is very small, phase transformation will occur spontaneously. On the other hand, if their stability is very high, $t\text{-ZrO}_2$ particles will not transform.

Metastable $t\text{-ZrO}_2$ can be obtained at room temperature (RT) and standard pressure by thermal treatment of the starting materials (zirconium salts, zirconium alkoxides or zirconium hydroxide), by ball-milling $m\text{-ZrO}_2$ ² and probably by ball-milling zirconium hydroxide,³ however the mechanism of its stabilization is still a matter of controversy.

The first mentioned mechanism of $t\text{-ZrO}_2$ stabilization emphasizes the influence of impurities remaining inside the crystal lattice during thermal treatment of the starting material.⁴ Davis⁵ showed that the pH value of the precipitated amorphous zirconium hydroxide influenced its thermal behavior. At low and high pH values, $t\text{-ZrO}_2$ was formed after calcination between 400 and 600 °C, while in neutral medium the same thermal treatment yielded $m\text{-ZrO}_2$. Štefanić *et al.*⁶ investigated the influence of the mechanical treatment on the thermal behaviour of zirconium hydroxide precipitated at different pH. It was found that, regardless of the precipitation pH, this influence can be present in the following way:



where T_{c1} , T_{c2} and T_{c3} stand for temperatures of crystallization mutually related $T_{c1} < T_{c3} < T_{c2}$.

High temperature X-ray diffraction measurements^{7,8} showed that zirconium hydroxide, regardless of the pH at which it precipitated, crystallized first as $t\text{-ZrO}_2$ that may or may not undergo transformation to $m\text{-ZrO}_2$ on cooling. Several other mechanisms of $t\text{-ZrO}_2$ stabilization emphasized the

role of particle size (surface energy),⁹ structural similarities between the starting material and *t*-ZrO₂,¹⁰ lattice strains,¹¹ water vapor,¹² oxygen vacancies,¹³ *etc.* However, experimental results concerning the low temperature *t*-ZrO₂ did not conform completely to the proposed mechanisms of stabilization. The difference between the cause(s) of *t*-ZrO₂ formation at RT and the causes of its stability is often neglected. The stability of low temperature *t*-ZrO₂ has not been studied intensively. Štefanić *et al.*¹⁴ investigated the products of thermal treatment of three different zirconium salts. The *t*-ZrO₂ fraction was the highest (almost 100%) for the sample obtained from ZrOCl₂•8H₂O salt, but that *t*-ZrO₂ was most sensitive to the temperature and pressure treatment. On the other hand, *t*-ZrO₂ obtained from Zr(SO₄)₂•4H₂O salt was shown to be most stable. It was concluded that the formation of *t*-ZrO₂ depended on the structure of the starting salt, and that the stability of the formed *t*-ZrO₂ was related to anionic impurities remaining in its crystal lattice.¹⁴ Srinivasan and co-workers¹⁵ concluded that oxygen-deficient surface sites initiated the transition *t*-ZrO₂→*m*-ZrO₂; the adsorption of SO₄²⁻ anions at these sites inhibited transition.

In our previous paper,¹⁶ we investigated the influence of SO₄²⁻ anions on the crystallization of zirconium hydroxide and the stability of the obtained metastable *t*-ZrO₂, subjected to the influence of temperature and pressure. It was found that the surface interaction between SO₄²⁻ anions and zirconia shifts the crystallization and the transition *t*-ZrO₂→*m*-ZrO₂ to a much higher temperature. The aim of the present work is to investigate the influence of precipitation pH values on the stability of metastable *t*-ZrO₂ subjected to temperature, pressure and γ -irradiation treatments. The suitability of laser Raman spectroscopy for determination of the volume fraction of *m*-ZrO₂ and *t*-ZrO₂ was also examined.

EXPERIMENTAL

Zirconium hydroxide was precipitated at pH 13, 7 and 2.5 from a solution of ZrO(NO₃)₂•2H₂O salt by addition of NaOH. The precipitates were separated from the mother liquor and then washed with doubly distilled water using a Sorvall RC2-B ultra-speed centrifuge (max. 20000 r.p.m.). In order to examine the influence of the washing procedure, we separated zirconium hydroxide precipitated at pH 2.5 into two parts. The first part was separated from the mother liquor and dried without previous washing. The second part was subjected to a washing procedure in the same manner as zirconium hydroxides precipitated at pH 7 and 13. After washing, the precipitates were dried at 100 °C for 24 hours. Dried gels were ground in an agate mortar for 2 minutes to insure a bigger yield of *t*-ZrO₂,⁶ and then calcined at 400 °C for 3 hours. Thus obtained starting samples Z13, Z7, Z2 and Z2A were subjected to the influences of temperature, pressure or γ -irradiation. Temperature treatment was performed by heating for 2 hours at 500 and 700 °C. The starting sample Z2 was also heated at 900 and 1100 °C. Pressure treatment was performed by subjecting the

starting samples for 2 minutes to a pressure of 500, 1000 or 1350 MPa using a Carver press. γ -irradiation of the starting samples Z13, Z7 and Z2 were performed using a cobalt-60 source at the Ruđer Bošković Institute at a dose rate of 5.6 Gy s^{-1} up to a final dose of 10 MGy. The notation of all the samples and the corresponding preparation conditions are given in Table I.

TABLE I

Names of the samples and the main experimental conditions.

Starting sample	Further treatment	Resulting ample
	–	Z13
	500 °C	Z13t1
Z13	700 °C	Z13t2
(precipitated at pH 13, 5 washing cycles, calcinated at 400 °C)	500 MPa	Z13p1
	1000 MPa	Z13p2
	1350 MPa	Z13p3
	10 MGy	Z13 γ
	–	Z7
	500 °C	Z7t1
	700 °C	Z7t2
Z7	500 MPa	Z7p1
(precipitated at pH 7, 5 washing cycles, calcinated at 400 °C)	1000 MPa	Z7p2
	1350 MPa	Z7p3
	10 MGy	Z7 γ
	–	Z2
	500 °C	Z2t1
	700 °C	Z2t2
	900 °C	Z2t3
Z2	1100 °C	Z2t4
(precipitated at pH 2.5, 5 washing cycles, calcinated at 400 °C)	500 MPa	Z2p1
	1000 MPa	Z2p2
	1350 MPa	Z2p3
	10 MGy	Z2 γ
	–	Z2A
	500 °C	Z2At1
Z2A	700 °C	Z2At2
(precipitated at pH 2.5, no washing, calcinated at 400 °C)	500 MPa	Z2Ap1
	1000 MPa	Z2Ap2
	1350 MPa	Z2Ap3

The phase composition of the obtained products was determined at RT by X-ray powder diffraction (Philips counter diffractometer, model MPD1880) and laser Raman (DILOR Z24) spectroscopy. XRD patterns were scanned in steps of 0.02° (2θ) with a fixed counting time of 5 s. The volume fractions of *m*-ZrO₂ and *t*-ZrO₂ were found from both XRD and laser Raman spectroscopy. In the case of XRD, the volume fractions were determined from the integrated intensities of lines $\bar{1}11$ and 111 of *m*-ZrO₂, and line 101 of *t*-ZrO₂ following the procedure proposed by Toraya *et al.*¹⁷ The volume fractions are given by the following equations:

$$v_m = \frac{1311x}{1 + 0.311x}, \quad v_t = 1 - v_m, \quad x = \frac{I_m(\bar{1}11) + I_m(111)}{I_m(\bar{1}11) + I_m(111) + I_t(101)}.$$

In the case of laser Raman spectroscopy the volume fractions were determined from the intensities of the Raman-active modes of *t*-ZrO₂ at 267 and 148 cm⁻¹, as well as the Raman-active modes of *m*-ZrO₂ at 189 and 178 cm⁻¹ following the procedure proposed by Clarke and Adar.¹⁸ The volume fractions of *m*-ZrO₂ were estimated from the following equation:

$$v_m = \frac{I_m^{178} + I_m^{189}}{F(I_t^{148} + I_t^{267}) + I_m^{178} + I_m^{189}},$$

where I_m and I_t correspond, respectively, to the intensities of the *m*-ZrO₂ and *t*-ZrO₂ Raman-active modes at the wave numbers, given as superscripts, while F is a factor close to unity (0.97).

The crystallite size was estimated using the Scherrer equation:

$$D = \frac{0.9\lambda}{\beta \cdot \cos\theta},$$

λ being the X-ray wavelength, θ the Bragg angle, β pure full width of the diffraction line at half the maximum intensity (FWHM). The values of β were found by applying a correction for the instrumental broadening, for which the corresponding width of the diffraction line 112 of α -SiO₂ was used, following the procedure given in the literature.¹⁹ The integrated intensities and FWHM of the diffraction lines were determined using the individual profile fitting method (computer program PROFIT).^{20,21}

RESULTS AND DISCUSSION

X-ray Powder Diffraction Patterns

The phase analysis of the starting samples Z13, Z7, Z2 and Z2A, as shown in Table II, indicates that in all four cases *t*-ZrO₂ is the dominant phase, and *m*-ZrO₂ is also present as the second phase. The biggest volume fraction of *m*-ZrO₂ (0.37) was present in sample Z7, and the smallest in sample Z2 (0.02). Nevertheless, in all four cases, the obtained crystallite sizes, determined from the diffraction lines 101 of *t*-ZrO₂ and $\bar{1}11$ of *m*-ZrO₂,

TABLE II

The results of phase analysis as determined by XRD and laser Raman spectroscopy.

Sample	XRD				laser Raman	
	Phase composition		Crystallite size/ nm		Phase composition	
	<i>t</i> -ZrO ₂	<i>m</i> -ZrO ₂	<i>t</i> -ZrO ₂	<i>m</i> -ZrO ₂	<i>t</i> -ZrO ₂	<i>m</i> -ZrO ₂
Z13	0.83	0.17	12.3	8.7	0.71	0.29
Z13t1	0.39	0.61	15.0	12.2	0.40	0.60
Z13t2	0.21	0.79	26.0	25.5	0.17	0.83
Z13p1	0.55	0.45	12.1	8.1	0.43	0.57
Z13p2	0.42	0.58	11.6	7.9	0.29	0.71
Z13p3	0.29	0.71	10.4	7.2	0.21	0.79
Z13γ	–	–	–	–	0.71	0.29
Z7	0.63	0.37	16.1	7.5	0.88	0.12
Z7t1	0.09	0.91	–	12.1	0.10	0.90
Z7t2	0.02	0.98	–	24.6	0.01	0.99
Z7p1	0.38	0.62	13.1	7.9	0.65	0.35
Z7p2	0.29	0.71	12.5	8.1	0.39	0.61
Z7p3	0.22	0.78	9.4	7.9	0.25	0.75
Z7γ	–	–	–	–	0.88	0.12
Z2	0.98	0.02	17.3	11.2	0.96	0.04
Z2t1	0.97	0.03	17.4	11.3	0.96	0.04
Z2t2	0.96	0.04	20.4	15.0	0.94	0.06
Z2t3	0.84	0.16	32.2	18.7	0.85	0.15
Z2t4	–	1.00	–	70.0	–	1.00
Z2p1	0.87	0.13	16.6	10.4	0.86	0.14
Z2p2	0.70	0.30	15.1	10.7	0.73	0.27
Z2p3	0.64	0.36	15.7	12.0	0.63	0.37
Z2γ	–	–	–	–	0.96	0.04
Z2A	0.91	0.09	9.4	7.3	0.70	0.30
Z2At1	0.73	0.27	11.2	9.7	0.48	0.52
Z2At2	0.53	0.47	13.9	16.5	0.36	0.64
Z2Ap1	0.62	0.38	9.5	7.4	0.49	0.51
Z2Ap2	0.50	0.50	9.7	7.9	0.40	0.60
Z2Ap3	0.42	0.58	9.7	8.1	0.32	0.68

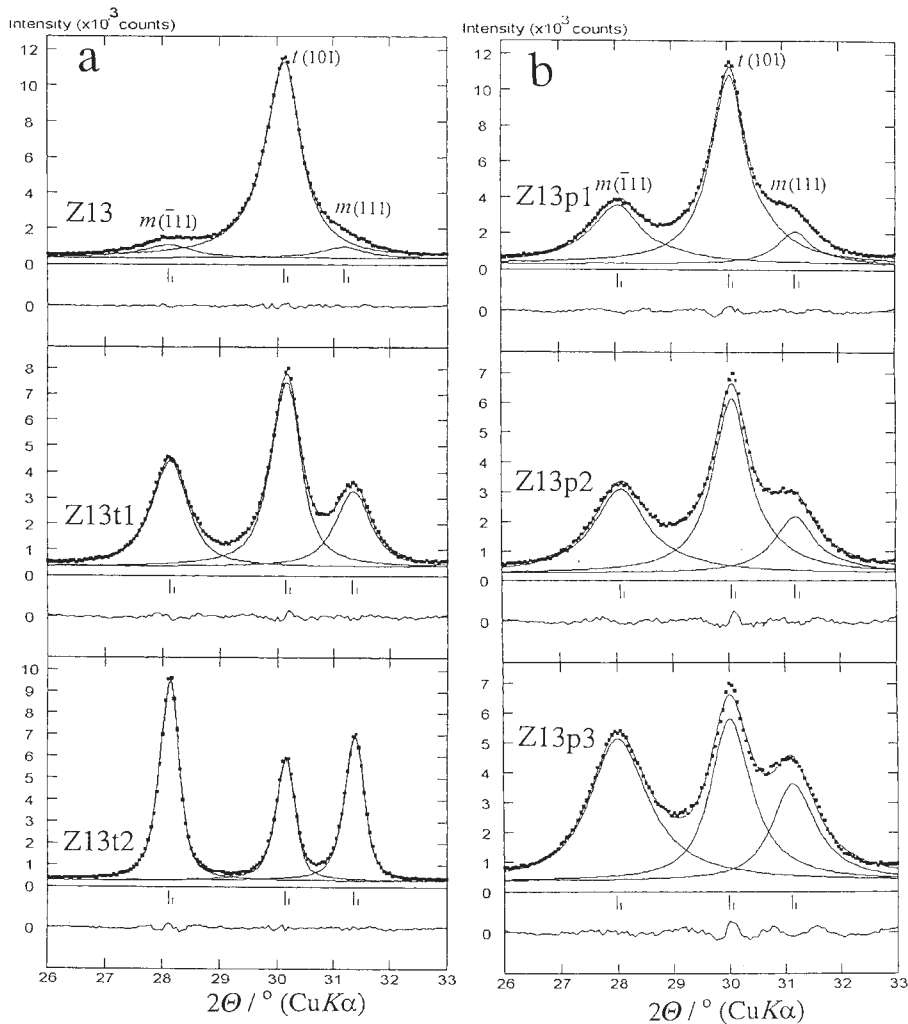


Figure 1. Individual profile fitting results of heated samples Z13, Z13t1 and Z13t2 (a) and pressure treated samples Z13p1, Z13p2 and Z13p3 (b).

are much smaller than the critical crystallite size (30 nm) as proposed by Garvie.⁹ The crystallite sizes of *t*-ZrO₂ were bigger than those of *m*-ZrO₂. Sample Z2A contained smaller crystallites than sample Z2, probably due to a loss of small particles during the washing procedure.

The individual profile fitting results of the samples obtained after the temperature and pressure treatment of samples Z13, Z7, Z2 and Z2A are shown in Figures 1, 2, 3 and 4. The obtained results of phase analysis are

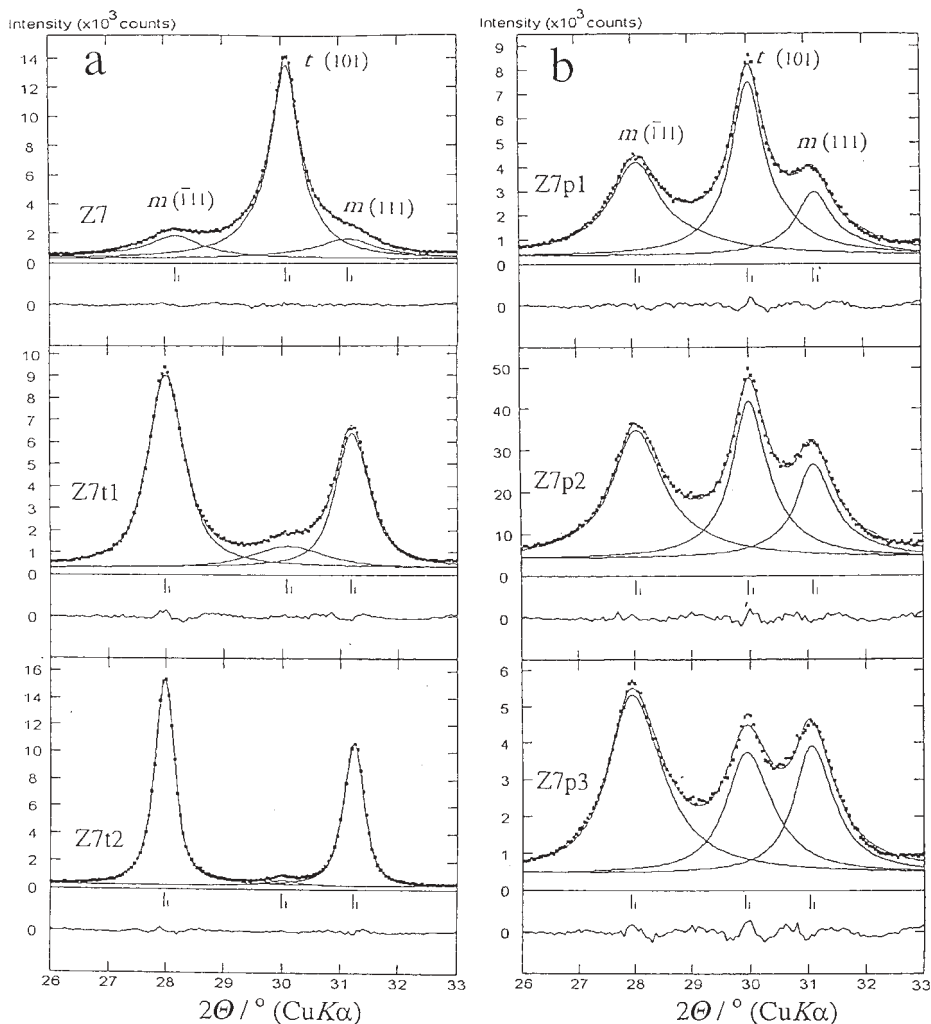


Figure 2. Individual profile fitting results of heated samples Z7, Z7t1 and Z7t2 (a) and pressure treated samples Z7p1, Z7p2 and Z7p3 (b).

summarized in Table II. In all cases, the increase in temperature or pressure caused a decrease in the volume fraction of metastable $t\text{-ZrO}_2$ and an increase in that of $m\text{-ZrO}_2$. In the case of temperature treatment, this process was accompanied by an increase in crystallite size (a decrease of the FWHM of diffraction lines). Although both $t\text{-ZrO}_2$ and $m\text{-ZrO}_2$ particles increased with the increase of temperature treatment, the crystallite size of $t\text{-ZrO}_2$ remained larger than those of $m\text{-ZrO}_2$ (with the exception of sample

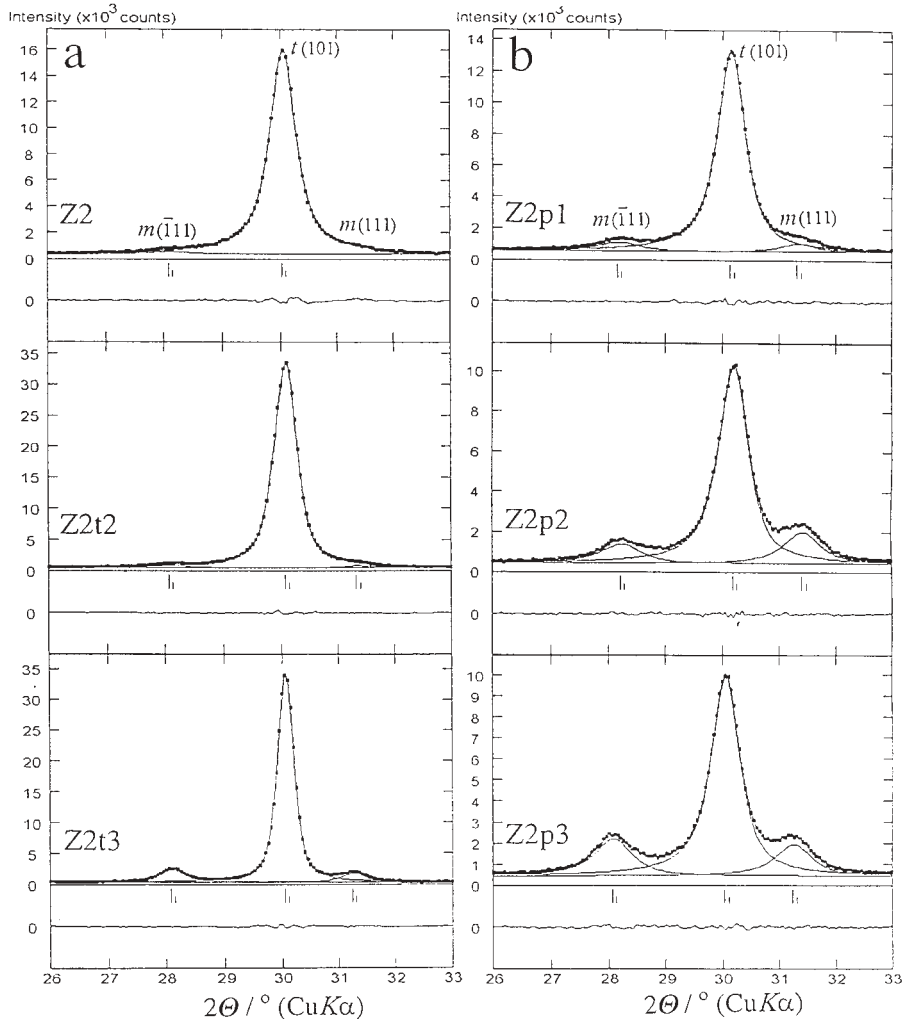


Figure 3. Individual profile fitting results of heated samples Z2, Z2t2 and Z2t3 (a) and pressure treated samples Z2p1, Z2p2 and Z2p3 (b).

Z2At2). The estimated crystallite size of t -ZrO₂ in sample Z2t3 (~32 nm) was close to the proposed critical crystallite size.⁹ The crystallite sizes of t -ZrO₂ and m -ZrO₂ in pressure treated samples remained approximately the same within the each series, indicating that in these cases crystallite size had very little influence on the transition t -ZrO₂→ m -ZrO₂. These results indicate that the crystallite size is not the only important factor in the formation of metastable t -ZrO₂. Avoidance of the washing procedure during the

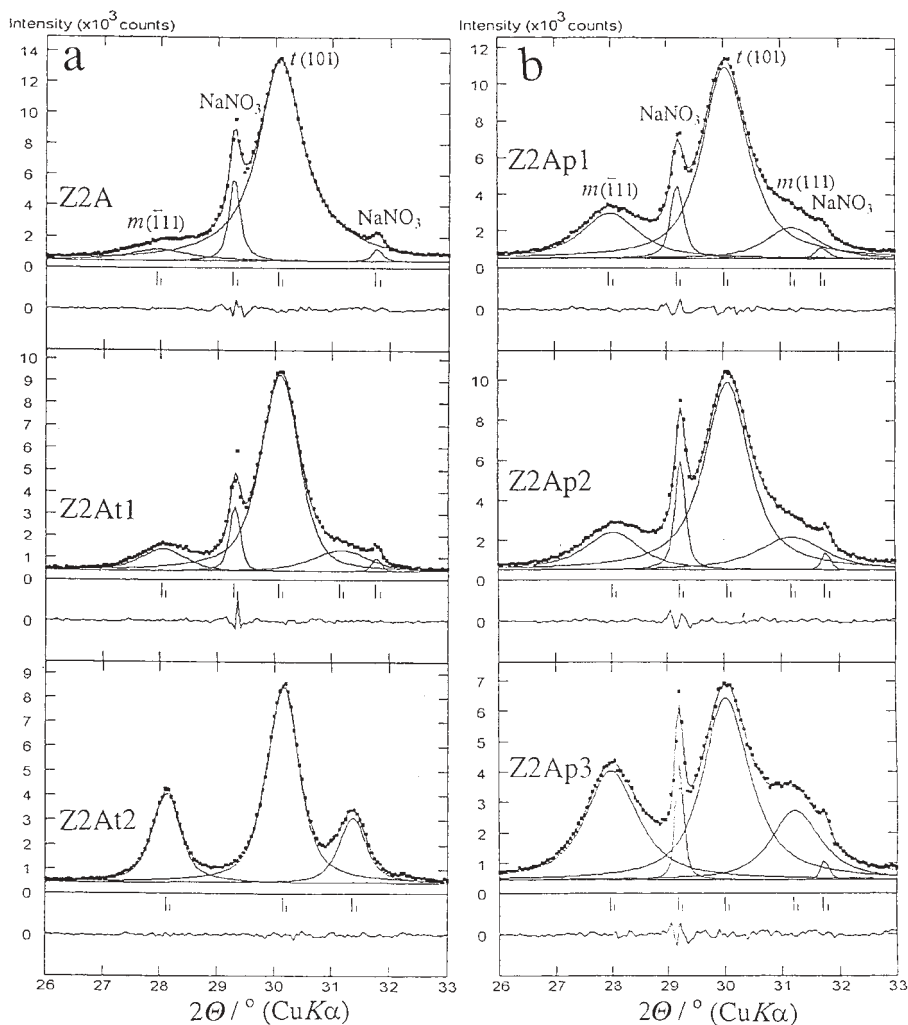


Figure 4. Individual profile fitting results of heated samples Z2A, Z2At1 and Z2At2 (a) and pressure treated samples Z2Ap1, Z2Ap2 and Z2Ap3 (b).

processing of sample Z2A caused the appearance of NaNO₃ as the third phase, besides *t*-ZrO₂ and *m*-ZrO₂, in samples Z2A, Z2Ap1, Z2Ap2, Z2Ap3 and Z2At1. After heating at a temperature of 700 °C (sample Z2At2), the diffraction lines of NaNO₃ disappeared.

Figure 5 shows how the volume fraction of the *m*-ZrO₂ of the starting samples Z13, Z7, Z2 and Z2A changed with the temperature increase. In all four cases, the fraction of the *m*-ZrO₂ phase increased with an increase in

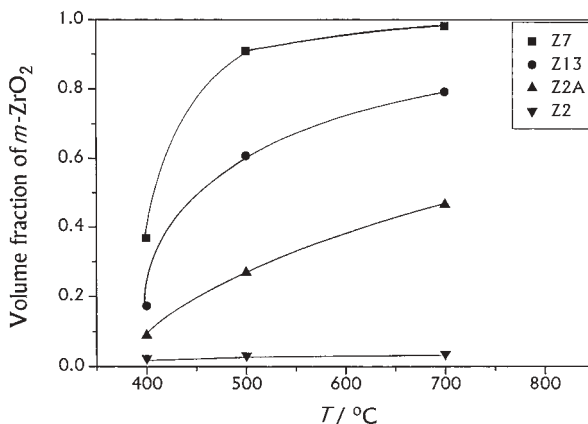


Figure 5. The m -ZrO₂ volume fraction of starting samples Z13, Z7, Z2 and Z2A as a function of temperature.

temperature, indicating the t -ZrO₂→ m -ZrO₂ transition. However, the rate of this transition was pH dependent. The metastable t -ZrO₂ has been shown to be most stable in sample Z2 (precipitated at pH 2.5) and most unstable in sample Z7 (precipitated at pH 7). The difference in stability was large; sample Z2, after heating at 700 °C, lost only 2% of the initial volume fraction of t -ZrO₂, while sample Z7 lost 97% of the initial volume fraction of t -ZrO₂ after the same treatment. Even after heating up to 900 °C sample Z2 lost only 14% of the volume fraction of t -ZrO₂ (Table II). The metastable t -ZrO₂ present in sample Z2A (also precipitated at pH 2.5) was shown to be more stable than the t -ZrO₂ present in samples Z7 and Z13 but much less stable than the t -ZrO₂ present in sample Z2. This result indicated that the washing procedure during the processing of the starting samples had an important influence on the stability of thus obtained t -ZrO₂. The shape of the obtained curves shows that the rate of the t -ZrO₂→ m -ZrO₂ transition decreased with the increase of the m -ZrO₂ content, indicating that the presence of the m -ZrO₂ phase hinders the transition of remaining t -ZrO₂. These results differ from the results of Srinivasan *et al.*²² The authors²² investigated the influence of the precipitation pH on the stability of t -ZrO₂ subjected to a temperature of 500 °C for different lengths of time. The obtained results indicate that the stability of metastable t -ZrO₂ increases with an increase in the precipitation pH. However, the stability of t -ZrO₂ obtained from zirconium hydroxide precipitated at pH 7, which in our case was shown to be most unstable, was not investigated. A major difference between our preparation procedure and the preparation procedure of Srinivasan *et al.*²² was in the grinding of dried gels. Our previous results showed that, regardless of the pH, brief ball-milling or grinding change amorphous zirconium hydrox-

ide in such a way as to produce metastable $t\text{-ZrO}_2$ after calcination at 400 to 600 °C.⁶ Without grinding, zirconium hydroxide precipitated at pH 7, after the same calcination procedure, yielded $m\text{-ZrO}_2$.^{5,6}

Figure 6 shows how the volume fraction of the $m\text{-ZrO}_2$ of the starting samples Z13, Z7, Z2 and Z2A changed with the increase in pressure. As in the case of the temperature treatment, the increase of pressure induced the $t\text{-ZrO}_2 \rightarrow m\text{-ZrO}_2$ transition. Stability of $t\text{-ZrO}_2$ has been shown to be pH dependent in the same way as in the case of temperature treatment (most stable in sample Z2 and most unstable in sample Z7), but in this case the difference in stability is not so pronounced. Sample Z2, after pressure treatment at 1350 MPa, lost 35% of the $t\text{-ZrO}_2$, while sample Z7, subjected to the same pressure, lost 65% of the $t\text{-ZrO}_2$. Also, the shapes of the obtained curves indicate that the presence of the $m\text{-ZrO}_2$ phase stabilizes the remaining $t\text{-ZrO}_2$ phase.

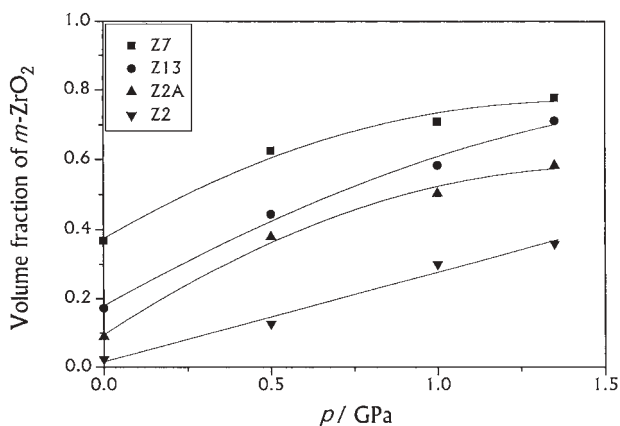


Figure 6. The $m\text{-ZrO}_2$ volume fraction of starting samples Z13, Z7, Z2 and Z2A as a function of pressure.

Laser Raman Spectroscopy

Laser Raman spectroscopy has been shown to be a very useful technique for determination of the ZrO_2 phase composition, especially when the cubic phase is present.^{23–25} However, its use in quantitative analysis has not been fully established. Clarke and Adar¹⁸ proposed a relation for determination of the $m\text{-ZrO}_2$ and $t\text{-ZrO}_2$ volume fractions, based on the fact that the laser Raman spectra of the $m\text{-ZrO}_2$ and $t\text{-ZrO}_2$ phases are characterized by sharp, strong and well separated bands. However, this relation was rarely used, with the exception of Hirata *et al.*^{25,26} On the other hand, quantitative analysis by XRD, using the relation proposed by Garvie and Nicholson²⁷

and Toraya,¹⁷ is very well established. In order to determine the capability of laser Raman spectroscopy for quantitative analysis, we compared the values of the *m*-ZrO₂ and *t*-ZrO₂ volume fractions determined by this technique with the corresponding values obtained by XRD.

Results of the phase analysis obtained by laser Raman spectroscopy showed, in agreement with the results of XRD, that *t*-ZrO₂ was the dominant phase in the starting samples Z13, Z7, Z2 and Z2A (Table II). The laser Raman spectra of γ -irradiated samples Z13g, Z7g and Z2g were approximately the same as the corresponding laser Raman spectra of nonirradiated samples Z13, Z7 and Z2. This result indicated that γ -irradiation had very little influence on the stability of metastable *t*-ZrO₂.

The laser Raman spectra of the samples obtained after the temperature and pressure treatments of starting samples Z13, Z7, Z2 and Z2A are given in Figures 7, 8, 9 and 10. The determined phase composition showed, in agreement with the results of XRD, that these treatments induced the *t*-ZrO₂ \rightarrow *m*-ZrO₂ transition (Table II). Also, the results of phase analysis indicated that the rate of this transition was pH dependent in the same way as it was estimated from the results of XRD.

Figure 11 shows the relation between the volume fraction of *m*-ZrO₂ determined by laser Raman spectroscopy using the method proposed by

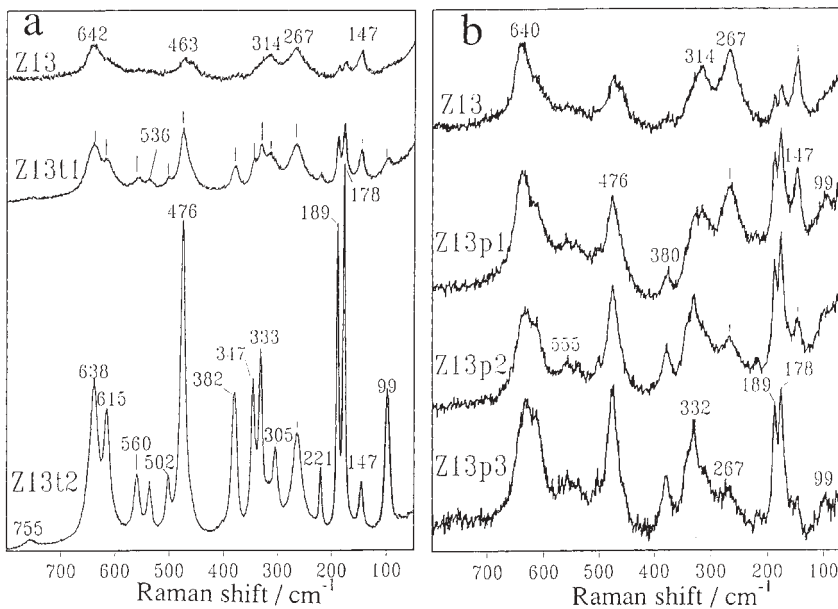


Figure 7. Laser Raman spectra of heated samples Z13, Z13t1 and Z13t2 (a) and pressure treated samples Z13, Z13p1, Z13p2 and Z13p3 (b).

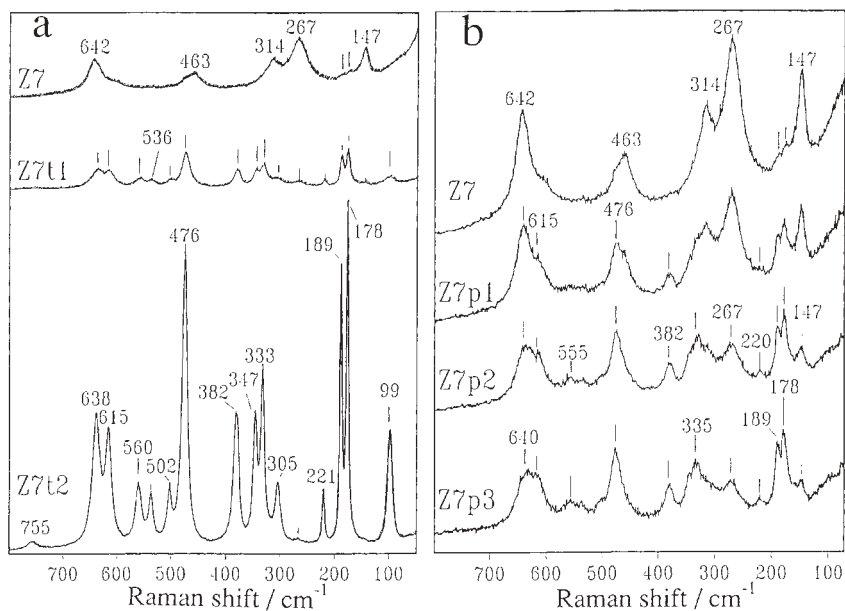


Figure 8. Laser Raman spectra of heated samples Z7, Z7t1 and Z7t2 (a) and pressure treated samples Z7, Z7p1, Z7p2 and Z7p3 (b).

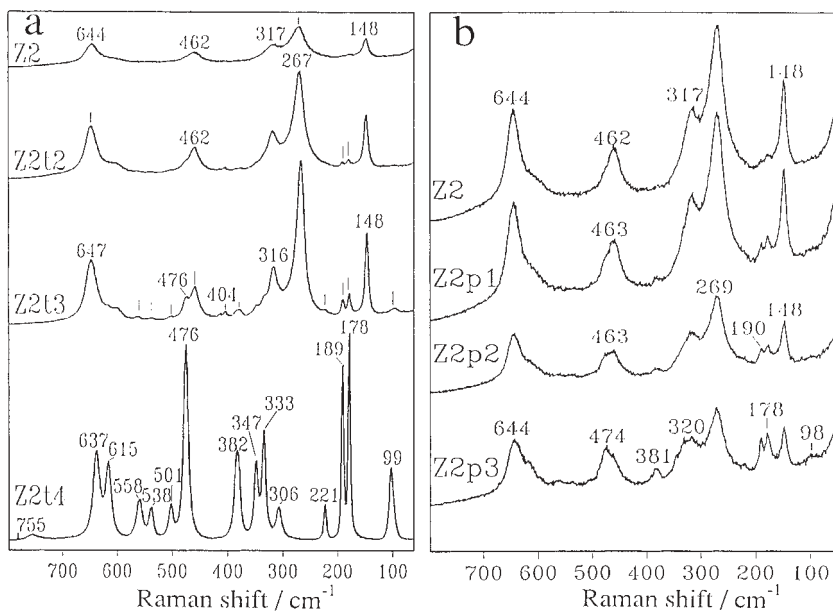


Figure 9. Laser Raman spectra of heated samples Z2, Z2t2, Z2t3 and Z2t4 (a) and pressure treated samples Z2, Z2p1, Z2p2 and Z2p3 (b).

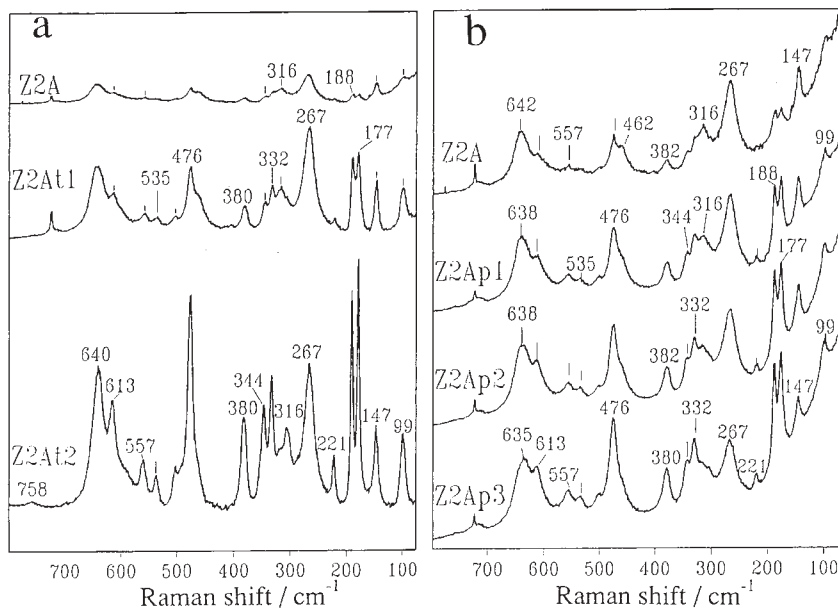


Figure 10. Laser Raman spectra of heated samples Z2A, Z2At1 and Z2At2 (a) and pressure treated samples Z2A, Z2Ap1, Z2Ap2 and Z2Ap3 (b).

Clarke and Adar¹⁸ and the volume fraction of *m*-ZrO₂ determined by XRD using the method proposed by Toraya.¹⁷ The obtained points are scattered around a dotted line, representing an ideal relation between the two techniques, in a way which indicates that the equation proposed by Clarke and Adar¹⁸ is correct. However, the obtained results show a non-uniform variance. The values of v_m estimated by laser Raman spectroscopy can be considered very reliable when $v_m > 0.70$ or $v_m < 0.15$. In the region $0.15 < v_m < 0.70$, the reliability of the estimated v_m values was much smaller. In the case of the samples obtained from the starting sample Z2A, the volume fraction of *m*-ZrO₂ was overestimated, while in the case of the samples obtained from the starting sample Z7, the volume fraction of *m*-ZrO₂ was underestimated. The observed differences probably result from heterogeneity in the phase composition of these samples (difference in the phase composition on the surface of the material as compared to the bulk of the material). It is well known that zirconium hydroxide precipitated at pH 7 and heated at ~400 °C yields *m*-ZrO₂.^{5,6} However, according to our previous work,⁶ brief ball-milling or even grinding of zirconium hydroxide caused *t*-ZrO₂ formation after heating at the same temperature. Also, it was shown that in shorter milling times only the outer part of the particles was affected.³ These affected parts of the grains produced *t*-ZrO₂ after the heating but the

unaffected parts inside the grains produced m -ZrO₂, resulting in an uneven distribution of crystalline phases through the grain. Laser Raman spectra are more influenced by the surface composition than by the composition of the bulk of the material.

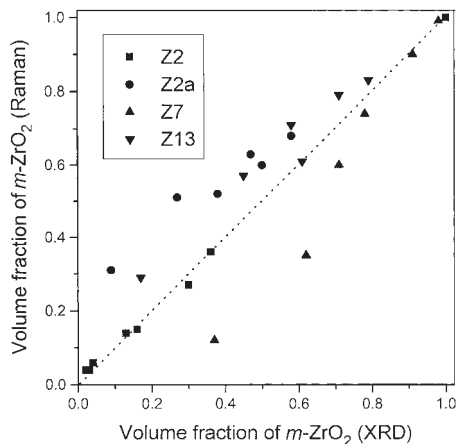


Figure 11. The relation between the m -ZrO₂ volume fraction determined by laser Raman spectroscopy using the method proposed by Clarke and Adar¹⁸ and the m -ZrO₂ volume fraction determined by XRD using the method proposed by Toraya.¹⁷

CONCLUSION

The results of phase analysis showed that a change in the pH of zirconium hydroxide precipitation caused a change in the sensitivity of the obtained metastable t -ZrO₂ under the influence of temperature and pressure. Metastable t -ZrO₂ obtained from zirconium hydroxide precipitated at pH 7 was most susceptible, while metastable t -ZrO₂ obtained from zirconium hydroxide precipitated at pH 2.5 was most stable. The rate of t -ZrO₂ → m -ZrO₂ transition decreased with the increase of the m -ZrO₂ content. The results of phase analysis obtained by laser Raman spectroscopy were compared with the corresponding results of XRD. It was concluded that the relation proposed by Clarke and Adar¹⁸ is correct. However, the capability of laser Raman spectroscopy for precise determination of the volume fraction of m -ZrO₂ and t -ZrO₂ is rather limited, especially for samples with an uneven distribution of crystal phases. It was found that all metastable t -ZrO₂ samples were stable under high γ -irradiation (10 MGy).

REFERENCES

1. Stevens, *Zirconia and Zirconia Ceramics*, Magnesium Electron Publication No. 113, Published by Magnesium Electron Ltd, July 1986, Printed by Litko 2000, Twickenham, U.K., pp. 17–19.
2. E. Bailey, D. Lewis, Z. M. Librant, and L. J. Porter, *Trans. J. Br. Ceram. Soc.* **71** (1972) 25–30.
3. G. Štefanić, S. Musić, and S. Popović, *Thermochim. Acta* **259** (1995) 225–234.
4. R. Cypres, R. Wollast, and J. Raucq, *Ber. Dtsch. Keram. Ges.* **40** (1963) 527–532.
5. B. H. Davis, *J. Am. Ceram. Soc.* **67** (1984) C–168.
6. G. Štefanić, S. Musić, and A. Sekulić, *Thermochim. Acta* **273** (1996) 119–133.
7. T. Mamott, P. Barnes, S. E. Tarling, S. L. Jones, and C. I. Norman, *J. Mater. Sci.* **26** (1991) 4054–4061.
8. R. Srinivasan, B. H. Davis, O. Burl Cavin, and C. R. Hubbard, *J. Am. Ceram. Soc.* **75** (1992) 1217–1222.
9. R. C. Garvie, *J. Phys. Chem.* **69** (1965) 1238–1243.
10. J. Livage, K. Doi, and C. Mazieres, *J. Am. Ceram. Soc.* **51** (1968) 349–353.
11. T. Mitsuhashi, M. Ichihara, and U. Tatsuke, *J. Am. Ceram. Soc.* **57** (1974) 97–101.
12. Y. Murase and E. Kato, *J. Am. Ceram. Soc.* **66** (1983) 196–200.
13. J. Torralvo, M. A. Alario, and J. Soria, *J. Catal.* **86** (1984) 473–476.
14. G. Štefanić, S. Musić, S. Popović, and K. Furić, *Croat. Chem. Acta* **69** (1996) 223–239.
15. R. Srinivasan, T. R. Watkins, C. R. Hubbard, and B. H. Davis, *Chem. Mater.* **7** (1995) 725–730.
16. G. Štefanić, S. Musić, S. Popović, and A. Sekulić, *J. Mol. Struct.* **408/409** (1997) 391–394.
17. H. Toraya, M. Yoshimura, and S. Somiya, *J. Am. Ceram. Soc.* **67** (1984) C119–C121.
18. D. R. Clarke and F. Adar, *J. Am. Ceram. Soc.* **65** (1982) 284–288.
19. H. P. Klug and L. E. Alexander: *X-ray Diffraction Procedures*, 2nd edition, John Wiley & Sons, New York, 1974, pp. 640–642, (Figure 9.9).
20. H. Toraya, *J. Appl. Cryst.* **19** (1986) 440–447.
21. B. Gržeta and H. Toraya, *Croat. Chem. Acta* **67** (1994) 273–288.
22. R. Srinivasan, R. De Angelis, and B. H. Davis, *J. Mater. Res.* **1** (1986) 583–588.
23. G. Štefanić, S. Popović, and S. Musić, *Thermochim. Acta* **303** (1997) 31–39.
24. R. Srinivasan, S. F. Simpson, J. M. Harris, and B. H. Davis, *J. Mater. Sci. Lett.*, **10** (1991) 352–354.
25. T. Hirata, E. Asari, and M. Kitajima, *J. Solid State. Chem.* **110** (1994) 201–207.
26. T. Hirata, *J. Phys. Chem. Solids* **56** (1995) 951–957.
27. R. C. Garvie and P. S. Nicholson, *J. Am. Ceram. Soc.* **55** (1972) 303–305.

SAŽETAK

Proučavanje stabilnosti niskotemperaturnog $t\text{-ZrO}_2$ primjenom rentgenske difrakcije u prahu i laser Raman spektroskopije

*Goran Štefanić, Svetozar Musić, Biserka Gržeta, Stanko Popović
i Andreja Sekulić*

Proučavan je utjecaj pH taloženja i prisutnosti kationa Na^+ na stabilnost metastabilnog $t\text{-ZrO}_2$. Uzorci cirkonijeva dioksida s velikim udjelom faze $t\text{-ZrO}_2$ dobiveni su kristalizacijom cirkonijeva hidroksida istaloženog pri pH 13, 7 i 2,5. Tako dobiveni uzorci podvrgnuti su utjecaju temperature, tlaka ili γ -zračenja, a fazni sastav dobivenih produkata određen je s pomoću rentgenske difrakcije na prahu i laserske Ramanove spektroskopije. Dobiveni rezultati pokazali su da promjena pH taloženja znatno mijenja osjetljivost metastabilnog $t\text{-ZrO}_2$ na utjecaje temperature i tlaka. Metastabilni $t\text{-ZrO}_2$ dobiven iz cirkonijeva hidroksida istaloženog pri pH = 2,5 pokazao se najstabilnijim, a metastabilni $t\text{-ZrO}_2$ dobiven iz cirkonijeva hidroksida istaloženog pri pH = 7, najosjetljivijim. Utvrđeno je da prisustnost kationa Na^+ smanjuje stabilnost metastabilnog $t\text{-ZrO}_2$. Svi su se uzorci pokazali stabilnima na utjecaj velike doze γ -zračenja. Mogućnosti laserske Ramanove spektroskopije u kvantitativnoj faznoj analizi proučavane su usporedbom vrijednosti volumnog udjela $m\text{-ZrO}_2$ (v_m) dobivenih tom tehnikom s odgovarajućim vrijednostima dobivenim primjenom rentgenske difrakcije na prahu. Utvrđeno je da je relacija koju su predložili Clarke i Adar, *J. Am. Ceram. Soc.* **65** (1982) 284., točna, ali pouzdanost vrijednosti v_m dobivenih laserskom Ramanovom spektroskopijom nije velika, posebno unutar koncentracijskog područja $0,15 < v_m < 0,70$. Razmatran je razlog niske pouzdanosti unutar tog područja.